Wind Engineering Joint Usage/Research Center
FY2013 Research Result Report

Research Field: Wind disaster and wind resistant design
Research Period: FY2013 ～ FY2014
Research Number: 133001
Research Theme: Equivalent Analysis on Wind-induced Vibration of Membrane Structures Considering Solid-fluid Interaction

Representative Researcher: Prof. Yuanqi Li

Budget [FY2013]: 560,000Yen

*If the research was not continuous, this will be the Final Result Report, so the contents of the report has to be detailed.
*There is no limitation of the number of pages of this report.
*Figures can be included to the report and they can also be colored.
*Submitted reports will be uploaded to the JURC Homepage.

1. Research Aim

This project mainly focuses on realization of numerical estimation on wind-induced vibration of membrane structures considering solid-fluid interaction with equivalent effect of air flow around membrane units in FE analysis. In FY2013, the main work is to establish numerical simulation framework for added mass estimation and to verify the suitability and efficiency of the proposed model by comparing between the added mass obtained from tests and numerical analysis. Some BLWT test will be conducted in FY2014.

2. Research Method

For numerical simulation, a singularity distribution method of distributing diploes on interfaces between fluid and structure will be developed to solve the problem of fluid flow induced by vibration of structures, and then the added mass can be expressed with the intensities of doublets, as well as the kinetic energy of the air flow around the curved membranes. Comparison between the added mass obtained from tests and numerical analysis will be done to verify the suitability and efficiency of the proposed model.

3. Research Result

3.1 Numerical analysis framework of still air induced by open flat membrane

A light open membrane structure of any shape in still air is considered. The membrane during vibration will induce the motion of surrounding air, and the air becomes a source of the additional inertia forces, as the same as the contribution of the structural mass. It is assumed that the air is incompressible and inviscid, and the velocity potential of the air satisfies the Laplace equation, i.e.,

$$\frac{\partial^2 \boldsymbol{\varphi}}{\partial x^2}+\frac{\partial^2 \boldsymbol{\varphi}}{\partial y^2}+\frac{\partial^2 \boldsymbol{\varphi}}{\partial z^2}=0 \tag{1}$$

where $\boldsymbol{\varphi}$ is the velocity potential of the air.

The solution of this equitation in integral form is

$$4\pi\frac{\partial \boldsymbol{\varphi}_P}{\partial \boldsymbol{n}_P}=\iint_{\Gamma_i}\boldsymbol{\varphi}_Q\frac{\partial^2}{\partial \boldsymbol{n}_P\partial \boldsymbol{n}_Q}(\frac{1}{\boldsymbol{r}_{PQ}})d\Gamma \tag{2}$$

where, $\boldsymbol{\varphi}_Q$ is the velocity potential of the air at point Q on the surface, $\boldsymbol{\varphi}_P$ is the velocity potential in any point of the space, $\boldsymbol{r}_{PQ}$ is the distance between any point P and a point Q on the surface (as Fig.1 shown), and $\frac{\partial \boldsymbol{\varphi}_P}{\partial \boldsymbol{n}_P}$ is the air velocity normal to the surface at the point P.

The boundary condition on the surface S is of Neumann's type and it is a coupling condition between the structure and the air. The formulations of the aerodynamic pressure and acceleration of the air are

$$\boldsymbol{p}_n = -\rho \frac{\partial \boldsymbol{\varphi}}{\partial t}, \quad \boldsymbol{a}_n = \frac{\partial^2 \boldsymbol{\varphi}}{\partial n \partial t} \tag{3}$$

where ρ is the air density.

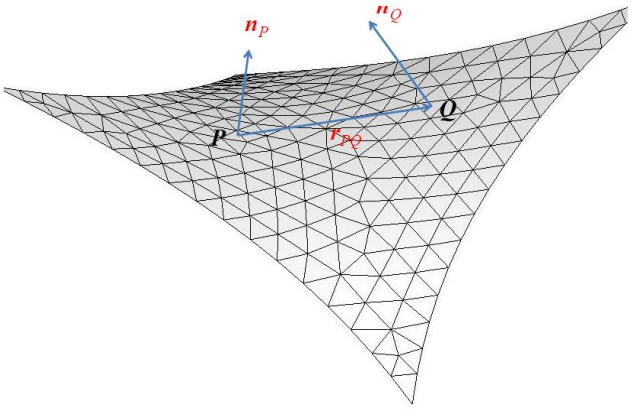

Fig.1 A light open membrane structure

Differentiating Eq.(2) with respect to time and using to Eq.(3) yields

$$-4\pi \boldsymbol{a}_{nP} = \iint_{\Gamma_i} \boldsymbol{p}_{nQ} \frac{\partial^2}{\partial \boldsymbol{n}_P \partial \boldsymbol{n}_Q} \left(\frac{1}{\boldsymbol{r}_{PQ}}\right) d\Gamma \tag{4}$$

where $\boldsymbol{p}_{nQ}$ is the resultant aerodynamic pressure acting at the point Q.

The BEM is used to numerically solve the boundary integral equation, Eq.(4). The surface of the membrane structure is discretized using the triangular elements. The boundary element discretization of Eq.(4) results in the following

$$-4\pi \boldsymbol{a}_n = \boldsymbol{A}\boldsymbol{p}_n \tag{5}$$

Here, the matrix $\boldsymbol{A}$, a $N \times N$ complex matrix (N is the number of triangular elements) is

$$\boldsymbol{A} = \iint_{\Gamma_i} \frac{\partial^2}{\partial \boldsymbol{n}_P \partial \boldsymbol{n}_Q} \left(\frac{1}{\boldsymbol{r}_{PQ}}\right) d\Gamma \tag{6}$$

The kernel of the integral has a strong singularity of the r^{-3} order, when the point Q approaches the point P ($\boldsymbol{r}_{PQ} \to 0$). For this case the integral cannot be directly determined. It can construct a set of related functions and use the Stokes formula to convert to the curvilinear integral on the edge of the surface. In this way, both the computational efficiency and accuracy are improved greatly.

The differentiation in Eq.(6) can be perform in the following form

$$\frac{\partial^2}{\partial \boldsymbol{n}_P \partial \boldsymbol{n}_Q} \left(\frac{1}{\boldsymbol{r}_{PQ}}\right) = \frac{-3z_P(x_Q - x_P)}{r_{PQ}^5} n_x + \frac{-3z_P(y_Q - y_P)}{r_{PQ}^5} n_y + \frac{-r_{PQ}^2 + 3z_P^2}{r_{PQ}^5} n_z \tag{7}$$

As shown in Fig.2, the local coordinate system of the element P is defined by (ξ, η, ζ). The direction of the unit axis vectors ζ is the unit normal vector of the element P. It can be derived as follow:

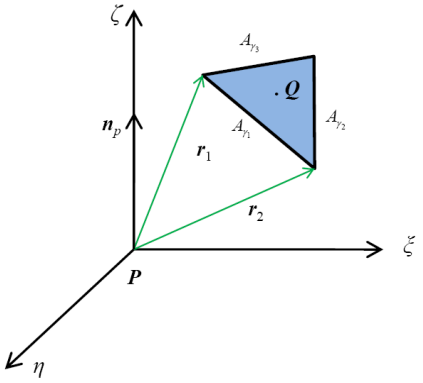

Fig.2 Local coordinate system of element P

$$\varsigma_1=\frac{-3z_P(x_Q-x_P)}{r_{PQ}^5}=\frac{-3\xi\zeta}{(\xi^2+\eta^2+\zeta^2)^{5/2}},\quad \varsigma_2=\frac{-3z_P(y_Q-y_P)}{r_{PQ}^5}=\frac{-3\eta\zeta}{(\xi^2+\eta^2+\zeta^2)^{5/2}},$$
$$\varsigma_3=\frac{-r_{PQ}^2+3z_P^2}{r_{PQ}^5}=\frac{\xi^2+\eta^2-2\zeta^2}{(\xi^2+\eta^2+\zeta^2)^{5/2}} \tag{8}$$

Denoting the function $M(\xi, \eta, \zeta)$, $N(\xi, \eta, \zeta)$, and $R(\xi, \eta, \zeta)$ as following

$$M=\frac{\eta}{(\xi^2+\eta^2+\zeta^2)^{3/2}},\quad N=\frac{\eta}{(\xi^2+\eta^2+\zeta^2)^{3/2}},\quad R=0 \tag{9}$$

Because

$$\frac{\partial M}{\partial\zeta}=\frac{-3\eta\zeta}{(\xi^2+\eta^2+\zeta^2)^{5/2}},\quad \frac{\partial M}{\partial\eta}=\frac{\xi^2+\zeta^2-2\eta^2}{(\xi^2+\eta^2+\zeta^2)^{5/2}},$$
$$\frac{\partial N}{\partial\zeta}=\frac{3\xi\zeta}{(\xi^2+\eta^2+\zeta^2)^{5/2}},\quad \frac{\partial N}{\partial\eta}=\frac{\xi^2+\eta^2-2\zeta^2}{(\xi^2+\eta^2+\zeta^2)^{5/2}} \tag{10}$$

and the relationships of the function P, Q, R and the potential function of the flow field are

$$\varsigma_1=\frac{\partial R}{\partial\eta}-\frac{\partial M}{\partial\zeta}\qquad \varsigma_2=\frac{\partial M}{\partial\zeta}-\frac{\partial R}{\partial\xi}\qquad \varsigma_3=\frac{\partial N}{\partial\xi}-\frac{\partial M}{\partial\eta} \tag{11}$$

According to the Stokes formula,

$$A_{ij}=\iint_{\Gamma_i}(\varsigma_1 n_x+\varsigma_2 n_y+\varsigma_3 n_z)dS=\iint_{\Gamma_i}[(\frac{\partial R}{\partial\eta}-\frac{\partial N}{\partial\zeta})n_\xi+(\frac{\partial M}{\partial\zeta}-\frac{\partial R}{\partial\xi})n_\eta+(\frac{\partial N}{\partial\xi}-\frac{\partial M}{\partial\eta})n_\zeta]dS$$
$$=\oint_{\partial\Gamma_i}Md\xi+Nd\eta+Rd\zeta=\oint_{\partial\Gamma_i}\frac{\eta d\xi-\xi d\eta}{(\xi^2+\eta^2+\zeta^2)^{3/2}} \tag{12}$$

Since the membrane is divided by triangle elements, so

$$\begin{cases}\xi(t)=\dfrac{\xi_2+\xi_1}{2}+\dfrac{\xi_2-\xi_1}{2}t=\dfrac{\xi_2+\xi_1}{2}+t\dfrac{\Delta\xi}{2}\\ \eta(t)=\dfrac{\eta_2+\eta_1}{2}+\dfrac{\eta_2-\eta_1}{2}t=\dfrac{\eta_2+\eta_1}{2}+t\dfrac{\Delta\eta}{2}\\ \zeta(t)=\dfrac{\zeta_2+\zeta_1}{2}+\dfrac{\zeta_2-\zeta_1}{2}t=\dfrac{\zeta_2+\zeta_1}{2}+t\dfrac{\Delta\zeta}{2}\end{cases} \tag{13}$$

Substitute Eq.(13) into Eq.(12), the curvilinear integral on the edge γ_1 can be derived as

$$A_{\gamma_1}=\oint_{\partial\Gamma_i}\frac{\eta d\xi-\xi d\eta}{(\xi^2+\eta^2+\zeta^2)^{3/2}}=\int_{-1}^{1}\frac{\eta(t)\xi'(t)-\xi(t)\eta'(t)}{[\xi(t)^2+\eta(t)^2+\zeta(t)^2]^{3/2}}dt=\int_{-1}^{1}\frac{2C}{(a+2bt+ct^2)^{3/2}}dt$$
$$=\frac{2C}{b^2-ac}\cdot(\frac{b-c}{\sqrt{a-2b+c}}-\frac{b+c}{\sqrt{a+2b+c}}) \tag{14}$$

where

$$C=(\eta_2+\eta_1)\Delta\xi-(\xi_2+\xi_1)\Delta\eta,\quad a=(\xi_2+\xi_1)^2+(\eta_2+\eta_1)^2+(\zeta_2+\zeta_1)^2,$$
$$b=(\xi_2+\xi_1)\Delta\xi+(\eta_2+\eta_1)\Delta\eta+(\zeta_2+\zeta_1)\Delta\zeta,\qquad c=\Delta\xi^2+\Delta\eta^2+\Delta\zeta^2 \tag{15}$$

Noting $\boldsymbol{r}_1=(\xi_1\quad\eta_1\quad\zeta_1)^T$, $\boldsymbol{r}_2=(\xi_2\quad\eta_2\quad\zeta_2)^T$, $\boldsymbol{r}_3=(0\quad 0\quad 1)^T$, Eq.(15) can be rewritten as

$$C=(\boldsymbol{r}_2-\boldsymbol{r}_1)\times(\boldsymbol{r}_1+\boldsymbol{r}_2)\cdot\boldsymbol{r}_3,\ a=(\boldsymbol{r}_2+\boldsymbol{r}_1)\cdot(\boldsymbol{r}_2+\boldsymbol{r}_1),\ b=(\boldsymbol{r}_1+\boldsymbol{r}_2)\cdot(\boldsymbol{r}_2-\boldsymbol{r}_1),\ c=(\boldsymbol{r}_2-\boldsymbol{r}_1)\cdot(\boldsymbol{r}_2-\boldsymbol{r}_1) \tag{16}$$

According to the invariance of the vector dot product and mixed product, we can use $\boldsymbol{r}_1$-$\boldsymbol{r}_j$ and $\boldsymbol{r}_2$-$\boldsymbol{r}_j$ substitute into $\boldsymbol{r}_1$ and $\boldsymbol{r}_2$ in the global coordinate system, and Eq.(16) can be rewritten as

$$C=(\boldsymbol{r}_2-\boldsymbol{r}_1)\times(\boldsymbol{r}_1+\boldsymbol{r}_2-\boldsymbol{r}_j)\cdot\boldsymbol{n}_j,\quad a=(\boldsymbol{r}_2+\boldsymbol{r}_1-2\boldsymbol{r}_j)\cdot(\boldsymbol{r}_2+\boldsymbol{r}_1-2\boldsymbol{r}_j),$$
$$b=(\boldsymbol{r}_2+\boldsymbol{r}_1-2\boldsymbol{r}_j)\cdot(\boldsymbol{r}_2-\boldsymbol{r}_1),\ c=(\boldsymbol{r}_2-\boldsymbol{r}_1)\cdot(\boldsymbol{r}_2-\boldsymbol{r}_1) \tag{17}$$

The curvilinear integral on the edge γ_1 , γ_2 and γ_3 can be derived in the same way, the elements A_{PQ} of the matrix $\boldsymbol{A}$ in Eq.(6) are given by

$$A_{PQ} = \sum_{k}^{3} A_{\gamma_k} \tag{18}$$

The resultant aerodynamic forces $\boldsymbol{P}_n$ acting at the centre of the ith element can be calculated as $P_{ni} = p_{ni}S_i$, where S_i is the area of the ith element. The relationship between the aerodynamic forces $\boldsymbol{P}$ acting on the nodes and the resultant aerodynamic forces $\boldsymbol{P}_n$ acting at the centre of the elements can be determined by

$$P_{rj} = \sum_{i=1}^{4} N_{ji} P_{ni} n_{ri} \tag{19}$$

where, P_{rj} is the rth component of force at node j, N_{ji} is the jth interpolation function at point i, n_{ri} is the rth component of the unit normal vector $\boldsymbol{n}_i$.

For the total system

$$\boldsymbol{P} = \boldsymbol{T}\boldsymbol{P}_n \tag{20}$$

where $\boldsymbol{T}$ denotes the transformation matrix.

The relationship between the acceleration of nodes $\boldsymbol{a}$ in the global coordinate system and the acceleration at the centre of the elements $\boldsymbol{a}_n$ is as follows:

$$\boldsymbol{a}_n = \boldsymbol{T}^T \boldsymbol{a} \tag{21}$$

(1) Determination of added mass according to effect of the geometric shape

Using the Eq.(6), (20) and (21), we can get

$$\boldsymbol{P} = \boldsymbol{M}_a \boldsymbol{a}_n \tag{22}$$

where the added mass matrix $\boldsymbol{M}_a = -4\pi \boldsymbol{T}\boldsymbol{S}\boldsymbol{A}^{-1}\boldsymbol{T}^T$.

The structural dynamic matrix equation can be obtained by means of FEM. The discretized equation of vibrations of the structure accounting for the aerodynamic forces is given by

$$\boldsymbol{K}_s \boldsymbol{u} + \boldsymbol{C}_s \dot{\boldsymbol{u}} + \boldsymbol{M}_s \ddot{\boldsymbol{u}} = \boldsymbol{P} \tag{23}$$

where $\boldsymbol{K}_S$ and $\boldsymbol{M}_S$ are the stiffness and mass metrics of the structure.

The equation of motion of an undamped dynamic system in matrix notation is

$$\boldsymbol{K}_s \boldsymbol{u} + (\boldsymbol{M}_s + \boldsymbol{M}_a)\ddot{\boldsymbol{u}} = 0 \tag{24}$$

In this method, the added mass is determined only by the membrane geometric shape, not the mode shape.

(2) Determination of added mass according to effect of the geometric shape and the mode shape

According to vibration theory, the structural vibration displacement can be separated into a modal vector and a set of generalized coordinates, i.e., the structural vibration displacement induced by the kth natural vibration can be expressed as

$$\boldsymbol{u}^{(k)} = \boldsymbol{\psi}^{(k)} \xi(t) \tag{25}$$

where $\boldsymbol{\psi}^{(k)}$ is the kth modal vector and $\xi(t)$ is a function of time.

The structural vibration velocity and acceleration induced by the kth natural vibration can be expressed as

$$\boldsymbol{v}^{(k)} = \frac{\partial \boldsymbol{u}^{(k)}}{\partial t} = \boldsymbol{\psi}^{(k)} \dot{\xi}(t), \quad \boldsymbol{a}^{(k)} = \frac{\partial^2 \boldsymbol{u}^{(k)}}{\partial t^2} = \boldsymbol{\psi}^{(k)} \ddot{\xi}(t) \tag{26}$$

And the resultant aerodynamic forces acting on the structure induced by the kth natural vibration can be expressed as

$$\boldsymbol{p}_n^{(k)} = \widehat{\boldsymbol{p}}_n^{(k)} \ddot{\xi}(t) \tag{27}$$

where $\widehat{\boldsymbol{p}}_n^{(k)} = -4\pi \boldsymbol{A}^{-1} \boldsymbol{\psi}^{(k)}$

In the case of an incompressible inviscid stationary fluid, the change rate in time of kinetic energy of any part of the fluid is equal to the work done by the pressures on its surface.

$$\frac{\partial E}{\partial t} = -\sum_{i=1}^{N} \int_S v_{ni} p_{ni} dS_i \tag{28}$$

where, E is the kinetic energy, and $\boldsymbol{v}_n$ denotes the velocity of the fluid particle in the direction of the normal $\boldsymbol{n}$. Assuming the fluid-solid interface of the membrane can be expressed as

$$\frac{\partial E}{\partial t} = -\sum_{i=1}^{N} \int_S \frac{\partial h_i}{\partial t} p_i dS_i \tag{29}$$

where, $\partial h / \partial t$ is the velocity of the membrane in the normal direction, $\boldsymbol{h}$ is the surface displacement of the membrane structure.

The change rate in time of the *k*th flow field kinetic energy induced by the *k*th natural vibration can be expressed as

$$\frac{\partial E^{(k)}}{\partial t} = -\dot{\xi}(t)\ddot{\xi}(t) \sum_{i=1}^{N} \int_S (\psi_i^{(k)} n_i) \hat{p}_i^{(k)} \, dS_i \tag{30}$$

where $\boldsymbol{n}$ is the normal direction of element.

On the other hand, the change rate in time of kinetic energy of the oscillating open membrane can be taken as the contribution of a equivalent mass per unit area, or the added mass, M_a, as described by

$$\frac{\partial E}{\partial t} = -M_a \sum_{i=1}^{N} \int_S \frac{\partial h_i}{\partial t} \frac{\partial^2 h_i}{\partial t^2} dS_i \tag{31}$$

For the *k*th natural vibration, Eq.(31) can be given

$$\frac{\partial E^{(k)}}{\partial t} = -\dot{\xi}(t)\ddot{\xi}(t) M_a^{(k)} \sum_{i=1}^{N} \int_S (\psi_i^{(k)} n_i)(\psi_i^{(k)} n_i) dS_i \tag{32}$$

So an expression for the added mass per unit area induced by the *k*th natural vibration can be given in the following form:

$$M_a^{(k)} = \frac{\sum_{i=1}^{N} \int_S (\psi_i^{(k)} n_i) \hat{p}_i^{(k)} dS_i}{\sum_{i=1}^{N} \int_S (\psi_i^{(k)} n_i)(\psi_i^{(k)} n_i) dS_i} \tag{33}$$

In this method, the added mass is determined by the membrane geometric shape, as well as the mode shape.

3.2 Analysis of added mass of circular membrane

A special vacuum chamber was designed by Li, et al (2011) to investigate the vibration of a circular flat membrane in still air with various air pressures. The membrane was clipped by a top circle and a bottom circle, and different prestress levels inside the membrane were imposed uniformly by lifting an inner circle. The vibration of the membrane was measured in 4 levels of air pressures, i.e., 1atm, 0.8atm, 0.6atm, and 0.35atm. Two membrane materials were used in the tests, including a latex and a rubber membrane, and five levels of prestress in the membrane were tested. Table 1 shows the test cases. Apparently, the natural frequencies of the membrane increase as air pressure decreases, as given in Table 2. Due to the arrangement of the displacement measuring points, the 3rd vibration mode of the latex membrane and the 4th vibration mode of the rubber membrane were lost. The fundamental frequency in vacuum was estimated by FEM, as listed in Table 3. With the obvious difference among the natural frequencies of the circular membrane vibrating in various air pressures and in vacuum, it can be seen that the added mass has a significant influence on the natural frequency of membrane structures.

The natural frequencies of the membrane considering the added masses are listed in Table 4. It can be seen that the result of the added mass model by Eq.(22) shows better agreement with the test results in the 1st mode, however, the error between the test results and the results with the added mass by Eq.(22) increases as the vibration mode increases. Generally speaking, the results with the added mass estimated by Eq.(33) are better agreement with the test results from 1st mode to 6th mode. Since the mass of the circle membrane is uniform, the mode shapes of the membrane vibrating in vacuum and with the added mass estimated by Eq.(33) are fully identical. In Fig.3, the difference of membrane mode shapes vibrating in vacuum and that with the added mass estimated by Eq.(22) is plotted together along the diameter. It is shown that the mode shapes with the added mass estimated by Eq.(22) has few changes.

Table 1 Test cases

Air pressure	Latex membrane			Rubber membrane	
	σ_1=0.092	σ_2=0.178	σ_3=0.297	σ_4=0.471	σ_5=0.828
1 atm	A1	B1	C1	D1	E1
0.8 atm	A2	B2	C2	D2	E2
0.6 atm	A3	B3	C3	D3	E3
0.35 atm	A4	B4	C4	D4	E4

Table 2 Natural frequency of the circular membrane vibrating in air with various pressures

Case	1st mode f_1 (Hz)	2nd mode f_2 (Hz)	3rd mode f_3 (Hz)	4th mode f_4 (Hz)	Case	1st mode f_1 (Hz)	2nd mode f_2 (Hz)	3rd mode f_3 (Hz)	4th mode f_4 (Hz)
A1	11.05	23.11	-	33.55	C3	24.34	49.31	-	78.91
A2	11.48	23.60	-	37.57	C4	30.96	58.95	-	92.00
A3	12.25	24.51	-	39.74	D1	35.58	67.42	97.38	-
A4	16.75	29.21	-	45.72	D2	36.83	69.91	99.25	-
B1	15.46	32.60	-	47.63	D3	39.95	73.04	-	-
B2	16.62	33.39	-	54.56	D4	45.57	78.65	107.4	-
B3	18.10	35.86	-	57.70	E1	51.20	97.38	151.1	-
B4	24.29	42.26	-	65.78	E2	51.81	97.69	-	-
C1	21.22	44.63	-	71.47	E3	53.99	102.4	-	-
C2	24.00	46.99	-	75.21	E4	63.98	111.7	-	-

Table 3 Natural frequencies of the circular membrane vibrating in vacuum

Prestress (MPa)	Finite Element Analysis				Fitting result of test			
	1st mode	2nd and 3rd mode	4th and 5th mode	6th mode	1st mode	2nd and 3rd mode	4th and 5th mode	6th mode
σ_1=0.092	24.45	39.08	52.48	56.43	24.45	33.38	-	61.96
σ_2=0.178	34.00	54.36	73.00	78.50	34.00	50.97	-	92.92
σ_3=0.297	43.98	70.02	82.50	101.39	43.98	72.18	-	110.18
σ_4=0.471	55.43	88.42	118.75	127.69	55.43	87.13	114.24	-
σ_5=0.828	73.49	117.24	157.45	169.30	73.51	121.13	-	-

Table 4 Natural frequencies of the circular membrane considering the added masses

Case	by Eq.(33)				by Eq.(22)			
	1st f_1 (Hz)	2nd& 3rd f_2 (Hz)	4th &5th f_3 (Hz)	6th f_4 (Hz)	1st f_1 (Hz)	2nd &3rd f_2 (Hz)	4th&5th f_3 (Hz)	6th f_4 (Hz)
A1	12.76	24.44	35.97	39.16	12.151	19.90	27.21	28.675
A2	13.81	26.08	38.05	41.36	13.186	21.568	29.455	31.073
A3	15.16	28.10	40.53	43.99	14.541	23.735	32.365	34.194
A4	17.59	31.44	44.44	48.09	17.019	27.653	37.595	39.848
B1	17.76	33.99	50.04	54.47	16.901	27.686	37.849	39.886
B2	19.21	36.28	52.92	57.54	18.342	30.001	40.971	43.221
B3	21.09	39.09	56.37	61.18	20.226	33.013	45.019	47.562
B4	24.47	43.73	61.81	66.90	20.226	33.013	45.019	47.562
C1	22.93	43.91	64.64	70.36	21.832	35.763	48.890	51.522
C2	24.81	46.86	68.36	74.32	23.692	38.753	52.923	55.829
C3	27.25	50.49	72.82	79.03	26.126	42.643	58.151	61.437
C4	31.61	56.49	79.84	86.41	30.579	49.686	67.549	71.597
D1	37.38	67.91	96.83	104.93	36.019	58.648	79.846	84.502
D2	39.61	70.88	100.25	108.51	38.301	62.244	84.633	89.693
D3	42.27	74.28	104.05	112.49	41.080	66.597	90.394	95.975
D4	46.52	79.30	109.49	118.13	45.585	73.568	99.561	106.07
E1	49.57	90.04	128.39	139.12	47.757	77.760	105.87	112.04
E2	52.51	93.98	132.92	143.87	50.783	82.529	112.21	118.92
E3	56.05	98.48	137.96	149.14	54.467	88.295	119.85	127.25
E4	61.68	105.14	145.17	156.63	60.440	97.542	132.01	140.63

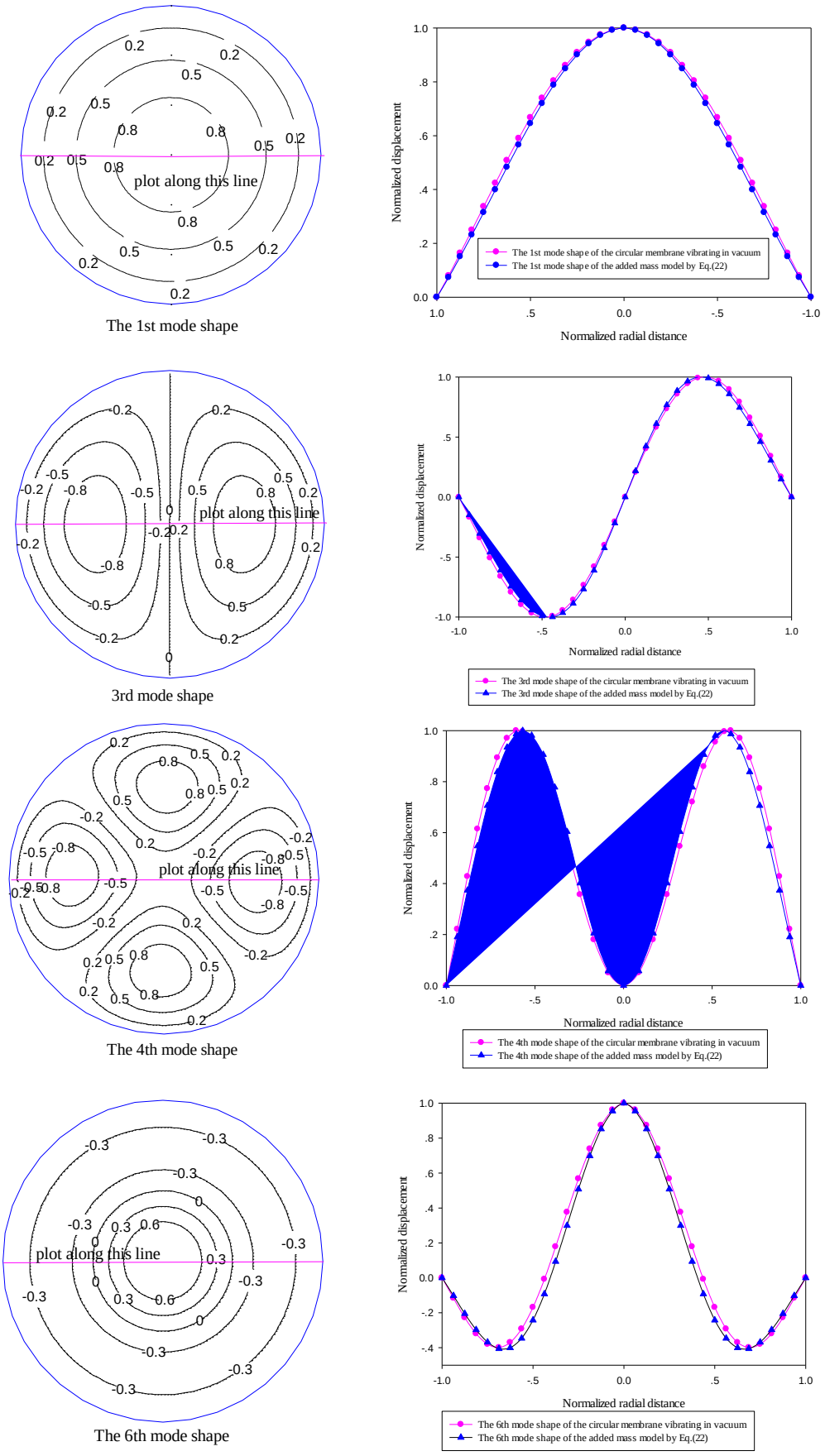

Fig. 3 Mode shapes of the circular membrane vibrating in vacuum and with the added mass by Eq.(22)

3.3 Analysis of added mass of square membrane

Experimental investigation of the first natural frequency of a square membrane was performed by R. Sygulski (1994). Fig. 4 shows the dimensions of the model. In theoretical calculations, the membrane was discretized to the boundary elements. The membrane cover was in form of the cable net with mesh 10 × 10 cm made of strand of 1.1 mm diameter, which was tensed by H = 68.67 N/m. The mass of the cover was represented by concentrated masses in nodes. The thin elastic film was attached to the net. To eliminate the influence of the added mass of air on vibration, the film was removed at first. Then, the net covered with film was used to reflect the membrane-air interactive system. In both cases, the mass distributed on the unit of the cover area was constant, 0.3 kg/m^2. The mass of the film was compensated by increasing the concentrated masses in nodes. The experimental result of the first natural frequency with film, or with air, was 5.88 Hz, and the result without air was 10.94 Hz. On the other hand, the result with the added mass estimated by Eq.(22) is 5.65Hz and that by Eq.(33) is 5.97Hz. Meanwhile, the first natural frequency in vacuum was estimated by FEM, and the result is 10.77 Hz. It can be found out that, in comparison with the experimental results in low mode, a good accuracy of the results obtained in numerical computation using two added mass models proposed in this paper can be achieved. As shown in Fig.5, there is little difference between the mode shapes vibrating in vacuum and the corresponding mode shapes with the added mass estimated by Eq.(22).

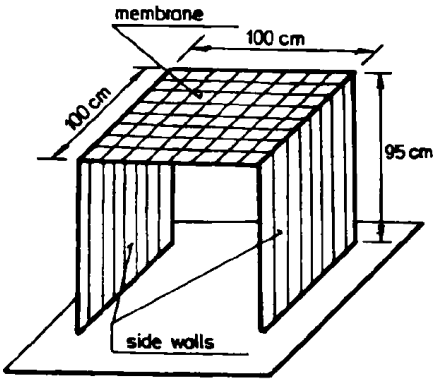

Fig. 4 A square membrane model (R. Sygulski, 1994)

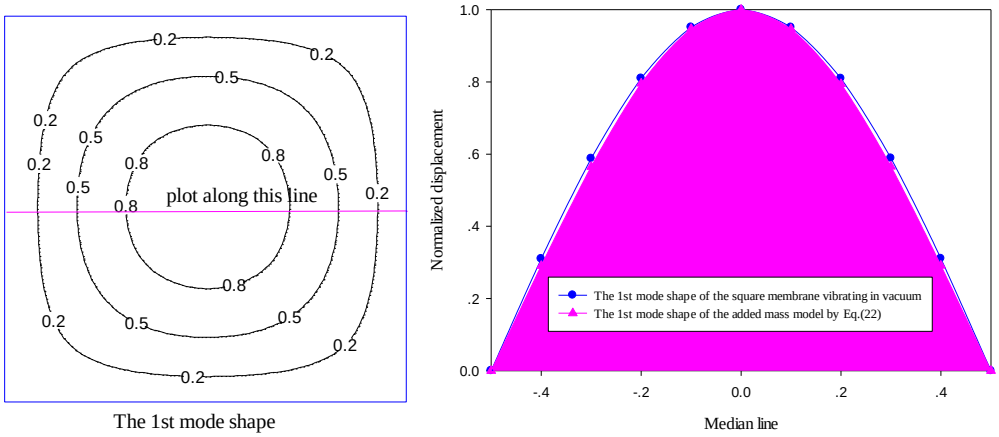

Fig. 5 Mode shapes of the square membrane vibrating in vacuum and with the added mass by Eq.(22)

3.4 Analysis of added mass of three-sided membrane

For the circular membrane and the square membrane, since the membrane mass is uniform, the mode shapes of the membrane vibrating in vacuum and with the added mass model estimated by Eq.(33) are fully identical. Hence, for the same vibration mode, the element of added mass is identical. Therefore, the determination of added mass using the added mass model by Eq.(33) is only based on the mode shape of the membrane vibrating in vacuum. However, when the mass distribution of the membrane is nonuniform, with the added mass model by Eq.(33) to calculate the added mass, the added mass determined by the effect of the mode shape will also influence the final mode shape of the membrane,

and a iteration analysis is necessary.

In this case, the analysis procedures of the added mass according to mode shape are as follows:

1) Calculate the natural frequencies and the mode shapes of the membrane vibrating in vacuum.
2) Use Eq.(33) to calculate the added mass.
3) For each vibration mode, calculate the natural frequencies and mode shapes of the membrane with the added mass estimated from Step 2.
4) Compare the natural frequencies and mode shapes of the membrane with that in the previous step. If they are close enough, then end off the iteration; Otherwise, calculate the added mass of the each element again based on the current mode shapes, and then repeat steps 2 through 4.

Sewall et al. (1983) investigated the vibration of a three-sided membrane both in vacuum and in still air, and tried to use as a surface reflective in space antennas. The membrane was designed as a three-sided membrane to obtain uniform prestress by tensioning the steel cables along the three-sided edges. The test set-up is shown in Fig. 5. The density of the membrane is 1384kg/m^3 and the density of the steel cable is 5500kg/m^3. Given the tension in the cable, the prestress in the membrane can be derived as:

$$\sigma = N / rt_{\mathrm{m}} \tag{34}$$

where, N is the tension in the cable, r is the radius of the curvature of the membrane, and t_{m} is the thickness of the membrane.

Test results on the natural frequencies of the three-sided membrane vibrating in still air are listed in Table 5. Sewall et al. (1983) also proposed a distribution model of the added mass of the membrane, as shown in Fig. 6. The natural frequencies of the membrane considering the added mass distribution proposed by Sewall are also listed in Table 5. It can be seen that the error between the test results and the model by Sewall is large and increases as the vibration mode increases. Table 5 also presents the natural frequencies of the membrane vibrating in still air based on the added mass model by Eq.(22) and by Eq.(33), respectively. It can be seen that the results with the added mass estimated by Eq.(22) shows better agreement with the test results in the 1st mode. However, the error increases as the order of vibration mode increases. It also can be seen that the results with the added mass estimated by Eq.(33) are quite satisfactory after the last iteration, with errors less than 5%. In this case, the mass distribution of the structure is nonuniform due to the steel cables. Hence, the mode shape of the structure vibrating in still air will be different from that in vacuum. As shown in Figs. 8, 9 and 10, the mode shapes vibrating in vacuum are different from that with the added mass estimated by Eq.(22) and Eq.(33). From Fig. 9 and Fig.10, it can be seen that the difference between the mode shapes of the three-sided membrane with the added mass estimated by Eq.(22) and that by Eq.(33) is little in the 1st, 2nd, 3rd, and 4th vibration modes, and a little larger in the 5th and 6th vibration modes.

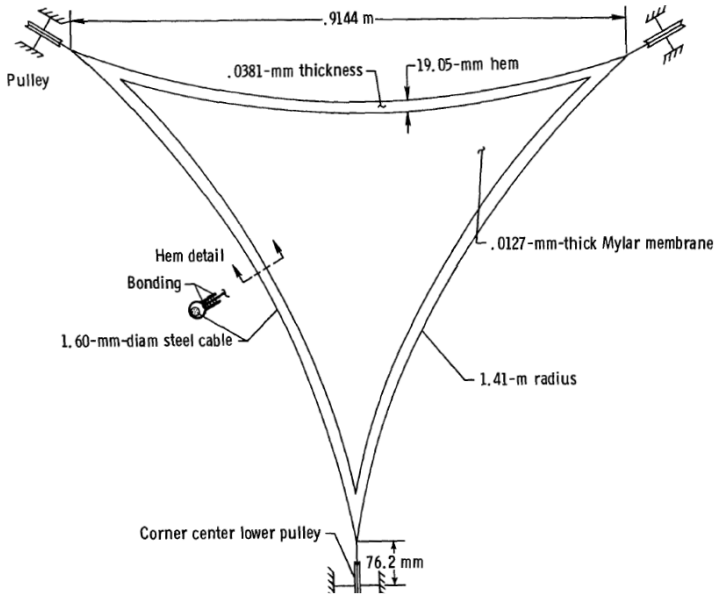

Fig. 6 Test setup for a three-sided membrane

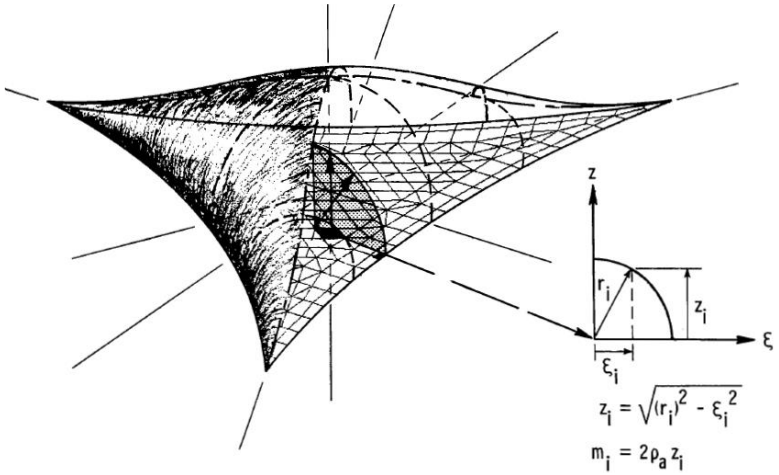

Fig. 7 The added mass distribution model proposed by Sewall

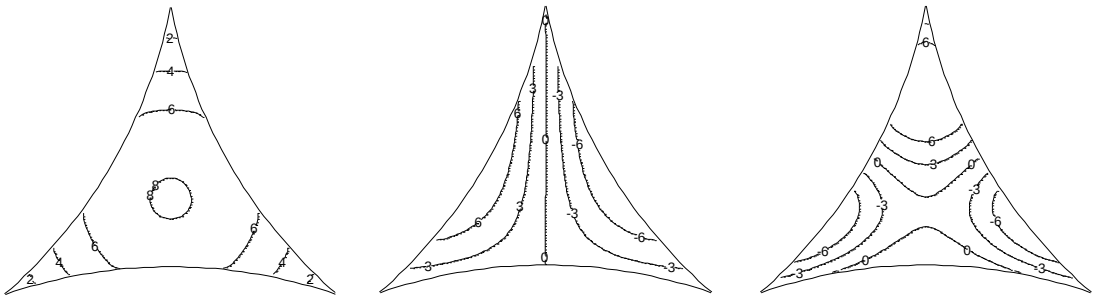

(a) 1st mode (b) 2nd mode (c) 3rd mode

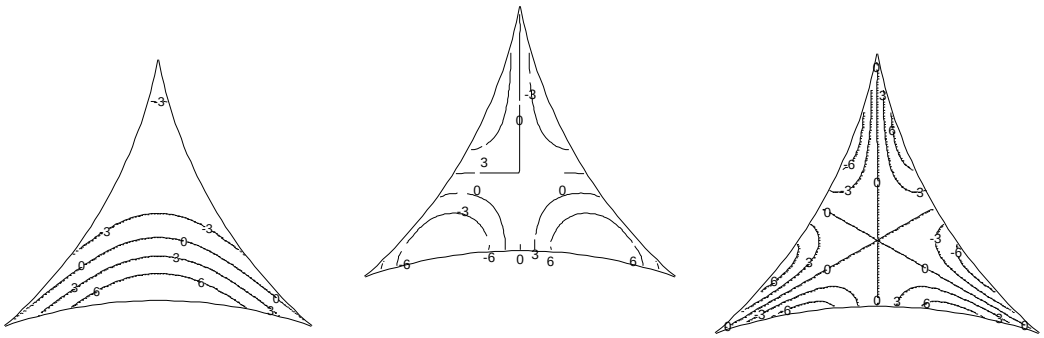

(d) 4th mode (e) 5th mode (f) 6th mode

Fig. 8 Mode shapes of the three-sided membrane vibrating in vacuum

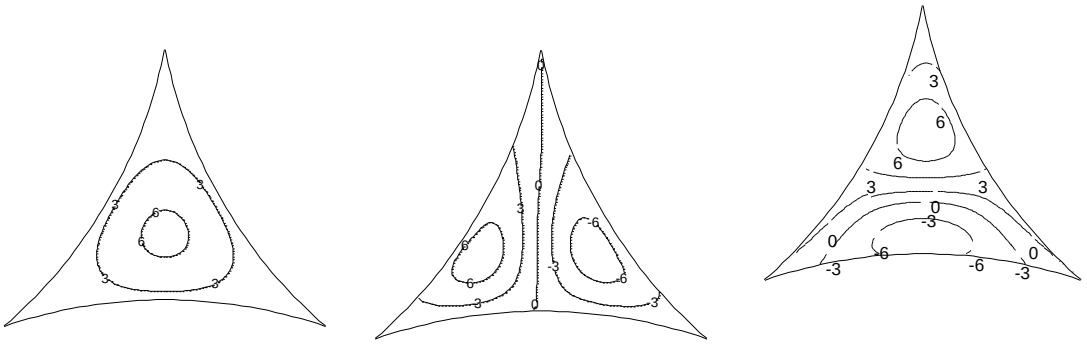

(a) 1st mode (b) 2nd mode (c) 3rd mode

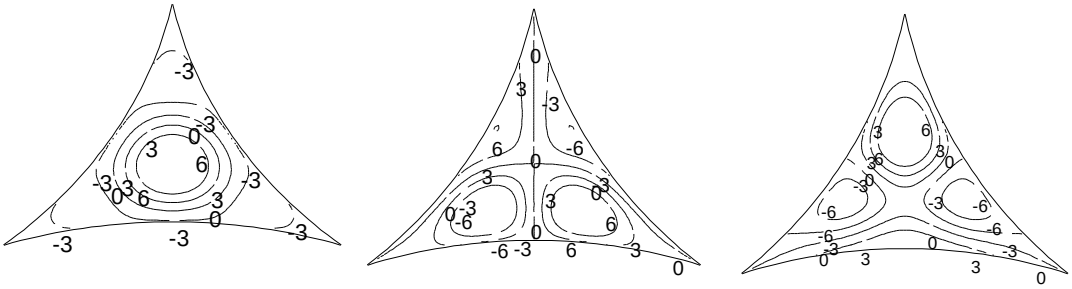

(d) 4th mode (e) 5th mode (f) 6th mode

Fig. 9 Mode shapes of the three-sided membrane with the added mass by Eq.(33) after the last iteration

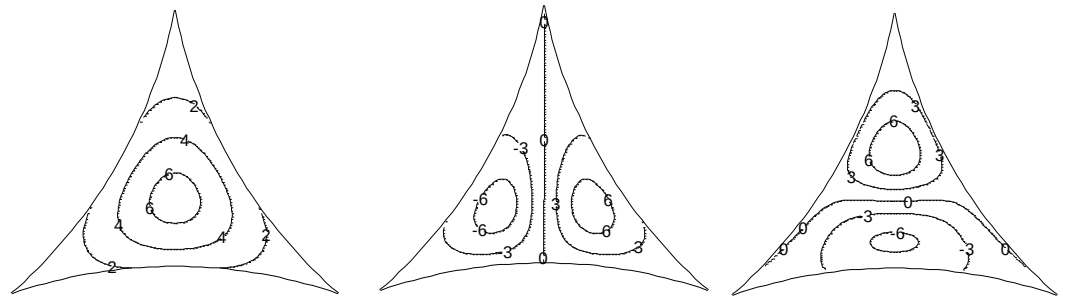

(a) 1st mode (b) 2nd mode (c) 3rd mode

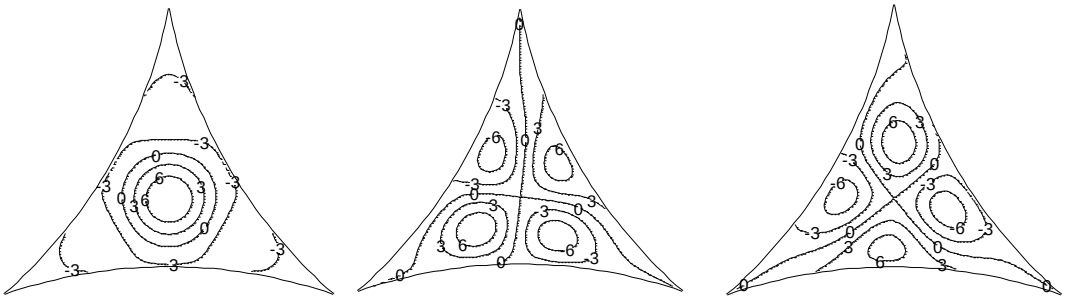

(d) 4th mode (e) 5th mode (f) 6th mode

Fig. 10 Mode shapes of the three-sided membrane with the added mass by Eq.(22)

Table 5 Natural frequencies of the three-sided membrane vibrating in still air (*N*=51N)

Mode	Test (Hz)	Model by Sewall (Hz)	Model by Eq.(22) (Hz)	Model by Eq.(33) (Hz)
1	13.94	12.73	14.18	14.38
2	26.34	23.09	24.35	28.63
3	28.90	23.26	24.35	30.57
4	34.77	27.36	29.75	35.73
5	43.14	34.83	36.22	45.94
6	43.85	34.92	36.22	46.21

* *N* is the prestress level in the membrane.

3.5 Conclusions

In this project, the boundary element method was applied to estimate the added mass for open flat membranes vibrating in still air. Two added mass models were proposed and discussed, one only considering the effect of the membrane geometric shape, and the other considering the effect of the geometric shape and the mode shape of membranes. The main findings were:

1) Added mass of air has a significant influence on the natural frequency of membrane structures in vibrating.
2) The proposed added mass model based on the effect of the geometric shape can have a good agreement with the test results in low-order modes, and the error will be increase as the order of vibration modes increases.
3) This proposed added mass model based on the effect of the geometric shape and the mode shape can have a better conformity with the test results both in low-order modes and high-order modes.
4) When the mass distribution of the membrane is uniform, the mode shapes of the membrane vibrating in vacuum as well as of the membrane with the added mass model according to geometric shape and mode shape are fully identical. There is little different between the mode shapes of the membrane with the added mass model according to geometric shape and the corresponding mode shapes of the membrane vibrating in vacuum.
5) When the mass distribution of the membrane is non-uniform, the mode shape of the structure vibrating in air will be quite different from that in vacuum. An iteration analysis is necessary with added mass model based on the effect of the geometric shape and the mode shape. Generally, it will be converged with several iterations. The difference between the mode shapes of the membrane with the added mass model according to geometric shape and the corresponding mode shapes with the added mass model according to geometric shape and mode shape is little in low modes and is large in some high modes.

Reference

Sygulski, R. (1994). Dynamic analysis of open membrane structures interacting with air. International journal for numerical methods in engineering, 37(11), 1807-1823.

Li Y.Q., Wang L., Shen Z.Y., Tamura Y., 2011. Added mass estimation of flat membranes vibrating in still air, Journal of Wind Engineering and Industrial Aerodynamics. 99, 815-824.

Sewall J.L., Miserentino R., Pappa R.S. 1983. Vibrating studies of a lightweight three-sided membrane suitable for space application. NASA Technical Paper, 2095.

4. Published Paper etc.

1) **Yi Zhou**, **Yuanqi Li***, **Zuyan Shen**, Lei Wang, **Akihito Yoshida** and **Yukio Tamura**, Numerical analysis of added mass for open flat membrane vibrating in still air using the boundary element method, Journal of Wind Engineering and Industrial Aerodynamics. (in modification after review)

2) **Yuanqi Li***, Lei Wang,**Yi Zhou** , **Zuyan Shen** and **Yukio Tamura**, Investigation on the added mass of flat membrane vibrating in still air, Seminar Lecture in Prof. Chen and Prof. Zuo's groups, TTU, Nov.29, 2013

5. Research workshop

東京工芸大学風工学共同研究拠点・TJU・TTU・共同研究集会, Seminar on Wind-resistant Design for Membrane Structures, National Wind Institute, Dept. of Civil and Environmental Engineering, Texas Tech University, Texas, USA, Nov.29, 2013

Table 6 Program of Seminar on Wind-resistant Design for Membrane Structures

Nov.29, 2013	Seminar	
13:30 - 13:45	Welcome Prof. Xinzhong Chen	Texas Tech University, USA
13:45 - 14:30	Prof. **Yuanqi Li*** Investigation on the added mass of flat membrane vibrating in still air	Tongji University, China
14:30 - 15:15	Mr. Jie Ding, Prof. Xinzhong Chen Assessing probabilistic load effects by simulation and statistical extrapolation	Texas Tech University, USA
15 minutes	Tea break	
15:30 - 16:15	Dr. Di Wu Uncertainty analysis in wind-resistant design of large-span spatial structures	Beijing Jiaotong University, China Visiting Scholar of TTU
16:15 - 17:15	Discussion	
16:15 - 17:15	Final comments and acknowledgements Prof. Yuanqi Li Prof. Xinzhong, Chen Prof. Delong Zuo	 Tongji University, China Texas Tech University, USA Texas Tech University, USA

Nov.30, 2013	Facilities visiting	
09:30 - 10:30	Boundary Layer Wind Tunnel Debris Impact Facility Tornado Simulator	Venue: Reese Center
10:30 - 12: 00	200m Meteorological Tower TTU Field Building	Venue: West of Reese Center

6. Research Organization

1. Representative Researcher

Yuanqi Li	Tongji University, China, Professor

2. Collaborate Researchers

Akihito Yoshida	Tokyo Polytechnic University, Japan, Associate Professor
Yukio Tamura	Tokyo Polytechnic University, Japan, Professor
Zuyan Shen	Tongji University, China, Professor
Akira Katsumura	Wind Engineering Institute Co., Ltd., Japan, Ph.D.
Yi Zhou	Tongji University, China, Ph.D. Candidate
Jun Ma	Tongji University, China, Ph.D. Candidate